

Blue-light-induced infrared absorption in KNbO₃

H. Mabuchi, E. S. Polzik, and H. J. Kimble

Norman Bridge Laboratory of Physics, California Institute of Technology, 12-33, Pasadena, California 91125

Received August 23, 1993; revised manuscript received May 24, 1994

We have used a high-finesse cavity to measure the cw intensity dependence and dynamics of blue-light-induced infrared absorption (BLIIRA) in KNbO₃ crystals for blue-light intensities between 7×10^{-4} and 2×10^4 W/cm². We discuss the detrimental effects of BLIIRA on the efficiency of intracavity frequency doubling and the threshold for parametric oscillation.

1. INTRODUCTION

Owing to its high nonlinearity and low passive losses, KNbO₃ has great potential as a medium for efficient frequency doubling and parametric oscillation.^{1,2} For example, KNbO₃ has been used successfully for the production of cw blue light by frequency doubling of a dye laser,³ doubling of a semiconductor diode laser,⁴ and nonlinear mixing of diode and Nd:YAG lasers.⁵ In recent work we observed 70% conversion efficiency for external cavity doubling of Ti:Al₂O₃ light near 860 nm and second-harmonic output power in excess of 0.6 W for 1.35 W of pump.^{6,7} We have also achieved parametric oscillation thresholds as low as 1 mW in an optical parametric oscillator (OPO) with KNbO₃.⁸ In principle even better performance should be possible—the measured crystal nonlinearity and passive intracavity losses of our current experimental setup imply a 90% conversion efficiency and oscillation threshold close to 200 μW. However, we have been prevented from achieving these values in practice by blue-light-induced infrared absorption (BLIIRA) in the crystal.^{6,9}

Phenomenologically, we define BLIIRA as the difference between the passive infrared absorption of a crystal and the infrared absorption that it exhibits when it is simultaneously illuminated by blue light. In the case of frequency doubling, the blue light is just the generated second-harmonic radiation, whereas in the process of parametric downconversion, BLIIRA is caused by the blue OPO pump. We have encountered BLIIRA in KNbO₃ for infrared wavelengths of 850–885 nm when the blue light is in the wavelength range 425–440 nm.

To quantify the detrimental effects of light-induced losses on the efficiency ϵ of external-cavity frequency doubling, we can write ϵ as

$$\epsilon = P_2/P_1 = [x + (x^2 + 1)^{1/2}]^{-2}. \quad (1)$$

This equation is valid for a ring cavity with optimized input coupler transmission, resonant for the fundamental wavelength only.¹⁰ Here, $x = L/2(EP_1)^{1/2}$, L gives the intracavity losses (passive + BLIIRA) excluding the input coupler transmission, E specifies the single-pass nonlinearity in W^{-1} , P_1 is the input power at the fundamental wavelength, and P_2 is the output power of

the second harmonic. The quantity E/L^2 may be considered a figure of merit for external-cavity frequency doubling; a strong, quadratic dependence on losses exists. In our current experiment, passive intracavity losses at fundamental wavelengths near 860 nm are as low as 0.35%. (By passive losses we mean the losses measured far from phase-matching conditions and without injected blue light.) Together with $E = 0.02$ W⁻¹ for our best 10-nm KNbO₃ crystal, Eq. (1) yields an expected efficiency $\epsilon > 90\%$ for $P_1 > 55$ mW. However, with BLIIRA of even 1% the efficiency drops to 67% at $P_1 = 55$ mW.

To realize the full potential of KNbO₃ for nonlinear optics, we need to understand and circumvent BLIIRA. With this goal in mind, we have studied BLIIRA in 10 different samples of KNbO₃ in order to characterize the effect and understand whether it is an intrinsic material property or is driven by impurities or other artifacts of a particular crystal growth process. In particular, we have measured the dependence of BLIIRA on the intensity of blue light, as well as the time response of BLIIRA. We have also investigated its sensitivity to temperature, applied electric field, and changes of the optical frequencies involved.

Our measurements of the intensity dependence of BLIIRA span seven orders of magnitude, from 7×10^{-4} W/cm² to 2×10^4 W/cm². The range that we have studied includes the intensity regime of interest for both cw frequency doubling and parametric oscillation. Several other studies of light-induced absorption at high intensities have previously been made in LiNbO₃:Fe,¹¹ BaTiO₃,^{12,13} and KNbO₃:Fe.¹³ However, these measurements were all made for homogeneous illumination of the crystal, whereas our measurements have been performed with focused, mode-matched beams, as appropriate for optimized nonlinear processes. Of particular relevance to this research is the study by Buse and Krätzig,¹³ who used a cw He–Ne laser to measure the absorption induced by nanosecond pulses from the second harmonic of a Q-switched Nd:YAG laser. We became aware of this research only after submitting this paper, so we find it interesting that these authors reached conclusions similar to ours, although they measured light-induced absorption in Fe-doped KNbO₃ crystals with different pump–probe wavelengths, different illumination conditions, and much

higher pump intensities than we have used. Several other studies of light-induced absorption processes in BaTiO₃ (Ref. 14) and Fe-doped KNbO₃ (Ref. 15) have been performed at relatively low intensities.

Many published studies on BaTiO₃ and KNbO₃:Fe discuss light-induced absorption in terms of a charge-transport model with two trapping levels. After presenting our results we will propose a simple modification that makes it possible to interpret the qualitative features of our data within the framework of this model.

Section 2 describes the setup we used for our measurements. Our BLIIRA measurement procedures and results are presented in Sections 3 and 4, and we conclude with a brief discussion and summary.

2. APPARATUS

We have investigated BLIIRA by using our homemade Ti:sapphire laser,⁷ KNbO₃-based external doubling cavity,⁷ and multipurpose KNbO₃ ring cavity⁹ (see Fig. 1). Our setup can be used to operate the ring cavity in three different modes, corresponding to frequency doubling, parametric oscillation, and pump-probe measurement of BLIIRA. Thus, we can measure both BLIIRA and nonlinear conversion efficiencies for a sample of KNbO₃ simply by changing the inputs to the ring cavity. This versatility allows us to verify directly that BLIIRA predominantly accounts for the anomalous intracavity losses, which we infer from our measurements of the conversion efficiency and parametric oscillation threshold of our ring cavity.

As illustrated in Fig. 1, our ring cavity is configured as a folded ring with two plane and two spherical mirrors

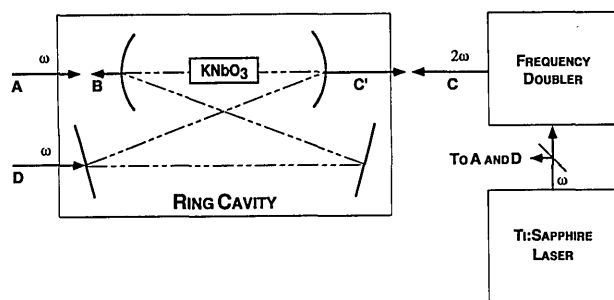


Fig. 1. Apparatus used to measure the cw intensity dependence of BLIIRA.

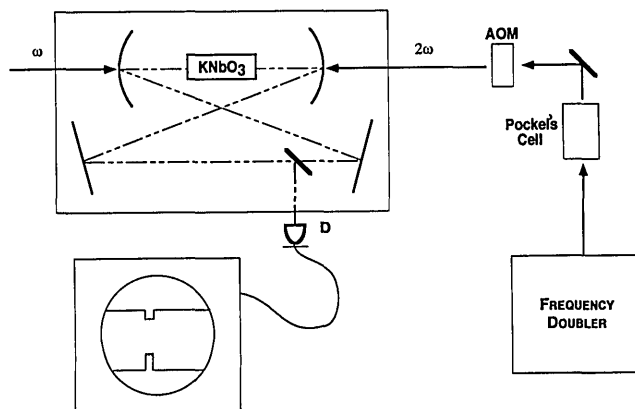


Fig. 2. Apparatus used to measure the time response of BLIIRA. AOM, acousto-optic modulator.

coated to build up infrared and transmit blue. A copper mounting block is used to hold an α -cut KNbO₃ crystal at the waist of the cavity mode. The mounting block and crystal are temperature stabilized to better than 0.01 °C by a Peltier cooler and feedback loop; for frequency doubling and parametric oscillation around 850–880 nm we perform noncritical phase matching. The width of the phase-matching curve for KNbO₃ is approximately 0.3 K, and the resonance frequency tunes about 0.5 nm/K. By measuring finesse, peak transmission, and the resonance dip in reflection from the input coupler, we were able to determine the total passive losses of our ring cavity. With our best KNbO₃ crystal in the cavity we measure $L_0 = (0.35 \pm 0.05)\%$.

To perform measurements of the frequency-doubling efficiency we pump the ring cavity with Ti:sapphire light (beam A) with beams C and D blocked and lock to an error signal derived from the reflection off the input coupler (FM locking¹⁶ with ± 27 -MHz sidebands generated by an electro-optic modulator). The second-harmonic output emerges as beam C'. When operated as an OPO, the ring cavity is pumped by blue light from the dedicated doubling cavity (beam C) with beam A blocked and is locked to a counterpropagating auxiliary IR beam from the Ti:sapphire (beam D). The IR output is beam B.

For BLIIRA measurements we tune off phase-matching conditions and pump the KNbO₃ crystal with blue light from the doubling cavity (beam C) and probe the induced IR absorption with a counterpropagating IR beam (beam A). We performed our cw power-dependence measurements by comparing the IR transmission of the ring cavity on resonance with and without injected blue light and computing from their difference the additional light-induced losses. During such measurements we were able to vary the crystal temperature by the use of the stabilized Peltier cooler, and for one of the crystals (which had a silver paint electrode) we could also apply electric fields along the c axis.

For our investigations of the BLIIRA time response we blocked one of the ring cavity mirrors and redirected the injected IR beam to a photodiode by the insertion of a pick-off mirror after the KNbO₃ crystal (see Fig. 2). Hence, the ring cavity was used only to facilitate precise mode matching of the blue pump and the IR probe beams beforehand and not as a resonator for enhancing measurement sensitivity. We generated pulses of blue light by sending the cw output of the doubling cavity through a Pockels cell and an acousto-optic modulator; two modulating elements were required in order to achieve adequate extinction of the blue light between pulses. We generally operated with extinction ratios around 10^{-5} , corresponding to pulses with peak power 100 mW and a dark level smaller than 1 μ W.

3. MEASUREMENTS OF THE CW INTENSITY DEPENDENCE OF BLUE-LIGHT-INDUCED IR ABSORPTION

As mentioned in Section 2, we measure light-induced losses in KNbO₃ by the observation of the drop in IR transmission of our ring cavity when blue light illuminates the crystal. To establish that the observed drop in the IR transmission is really due to light-induced

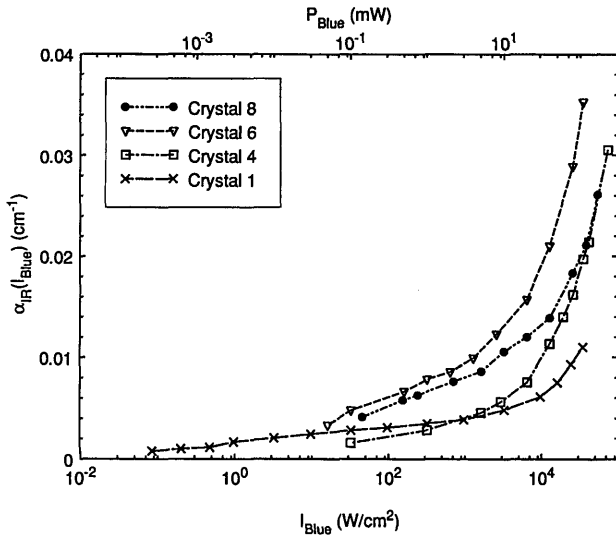


Fig. 3. BLIIRA cw intensity-dependence curves for four different KNbO_3 crystals. We denote $\alpha_{\text{IR}}(I_{\text{Blue}})$ the BLIIRA as a function of blue-light intensity.

absorption rather than scattering, refraction, or some phase-matched nonlinear process, we performed several additional tests.

First, the effect proved to be independent of the relative directions of propagation of the blue and the IR beams. As the observations are carried out far from the phase-matching temperature for frequency doubling, this independence essentially rules out the possibility of any parametric interaction being responsible for the anomalous IR losses.

To check the possibility of the IR beam's being refracted (e.g., by the photorefractive effect) or otherwise spatially distorted (e.g., by thermal lensing) in the presence of blue light, we analyzed the spatial shape of the beam transmitted through the KNbO_3 ring cavity by interfering it with a TEM_{00} reference beam of very high quality. We found the fringe visibility of 99.2% obtained without blue light to be practically unchanged when the crystal was illuminated by 200 mW of blue light. Our visibility measurement accuracy was 0.1%, corresponding to an uncertainty of 0.2% with regard to changes in the spatial distribution of IR energy circulating in the KNbO_3 ring cavity.

Finally, to detect the absorption directly we made calorimetry measurements. The temperature of the crystal was measured first with and then without the IR light passing through. The difference δT_0 due to absorptive

heating was compared with the corresponding quantity δT measured in the presence of the blue beam. The measured value of δT was several times higher than δT_0 , demonstrating that light-induced losses in KNbO_3 are mainly due to IR absorption.

For our measurements of BLIIRA at high blue-light intensities the injected blue beam C (Fig. 1) is focused and mode matched to the circulating IR beam. We achieve alignment by producing blue light in the ring cavity (see above) and mode matching both this beam, C', and the injected blue beam, C, to an auxiliary cavity. Thus the beam geometry used in our high-intensity BLIIRA measurements is identical to that used for frequency doubling and parametric oscillation in our ring cavity in the sense that the blue beam waist was $2^{1/2}$ times smaller than the IR beam waist and both beams were precisely mode matched. In particular, the waist of the cavity mode coincides with the optimal waist for frequency doubling. However the crystal temperature was completely detuned from phase matching in order to suppress all $\chi^{(2)}$ nonlinear-optical processes.

For measurements with low blue-light intensity we removed the mode-matching lens at the blue-light input of the ring cavity and illuminated the crystal with an approximately parallel beam of 2-mm diameter.

In all we tested 10 KNbO_3 crystals, including one Fe-doped crystal [dopant level 50 parts in 10^6 (ppm)] and one MgO-doped crystal (dopant level 0.1%). Nine of the ten crystals were grown and polished by Virgo Optics, and the tenth was grown by Sandoz (France) and polished by Virgo Optics. There is a large variation of the cw power dependence of BLIIRA from sample to sample—representative curves are shown in Fig. 3. The $\text{KNbO}_3:\text{MgO}$ crystal exhibited rather high BLIIRA, whereas the Fe-doped sample was not significantly different from nominally pure crystals. Our measurements of BLIIRA and some passive optical properties of eight KNbO_3 crystals studied in this work are summarized in Table 1.

One crystal showed a strong sensitivity to temperature; curves taken at 10 °C and 70 °C are shown in Fig. 4. The other crystals that we tested did not exhibit any observable temperature dependence of BLIIRA within the range 10–100 °C. One of our undoped crystals had a silver paint electrode that allowed us to apply electric fields across the *c* axis. dc fields up to 1 kV/3 mm did not have any detectable effect on the level of BLIIRA induced by cw blue light.

Table 1. Summary of KNbO_3 Crystal Parameters

Crystal	Length (mm)	E_{NL} (W^{-1})	Passive Losses		BLIIRA (cm^{-1}) at 100 mW of Blue (30 kW/cm^2)
			860-nm Bulk/Surf	430-nm Bulk/Surf	
Crystal 1	10	0.018	0.45% total	4%/4%	1.1%
Crystal 2	15	0.029	1.1% total	24%/0.7%	2.7%
Crystal 3 (MgO)	15	0.021	0.9% total	8%/1.4%	8.0%
Crystal 4 (b-Growth)	15	0.018	0.55%/0.1%	6%/4.5%	1.9%
Crystal 5 (Fe)	10	—	—	—	2.5%
Crystal 6 (Sandoz)	11	—	—	—	3.3%
Crystal 7	20	—	—/1.4%	—	1.1% at 70 °C 3.5% at 10 °C
Crystal 8	18	—	—	—	2.0%

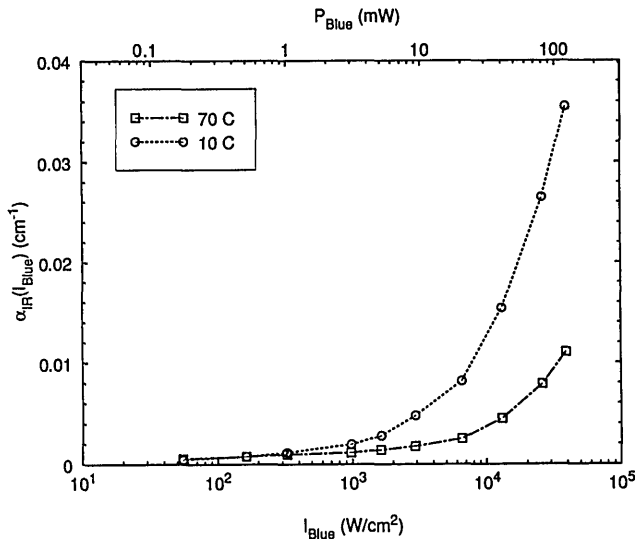


Fig. 4. Anomalous temperature dependence of BLIIRA in one KNbO_3 sample.

We made one set of precise measurements on our best KNbO_3 crystal (the one with the smallest BLIIRA). Results for the high- and low-intensity measurements are shown in Fig. 5 on both log–lin and log–log scales. These data were taken with a 3 mm \times 3 mm \times 10 mm KNbO_3 crystal held at 40°C. High precision was achieved by the replacement of the usual 10% transmission input coupler of the KNbO_3 with a high reflector ($R = 0.99989$). We estimate our point-to-point measurement error to be approximately 5×10^{-5} , and there is an uncertainty of 10% in the overall normalization of the curve. The overall shape of the curve in Fig. 5(b) strongly suggests that there are two regimes of the BLIIRA intensity dependence. One might speculate that the resurgence of BLIIRA above approximately 5 kW/cm² could be due to the existence of a secondary light-induced absorption mechanism that can only be activated by relatively high intensity of blue light. This hypothesis is corroborated by our measurements of the BLIIRA time response, which are described in Section 4.

All the measurements described thus far were made with the Ti:sapphire laser tuned to 860 nm, corresponding to a blue-light wavelength of 430 nm. For our best crystal we also measured the BLIIRA cw power dependence with 880-nm IR light and 440-nm blue light. A graph of these data is shown in Fig. 6. The curves seem to match fairly well at higher intensities, but at lower intensities the light-induced absorption is smaller for the longer set of wavelengths. This result suggests that the secondary mechanism mentioned above couples equally well to the two wavelengths used, whereas the primary mechanism is wavelength dependent with lower absorption at higher wavelengths (we will return to this point in our conclusions).

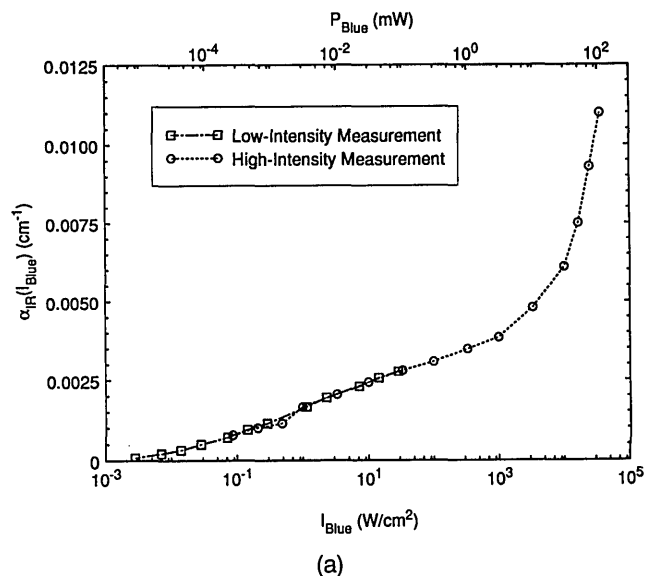
4. MEASUREMENTS OF THE BLUE-LIGHT-INDUCED IR ABSORPTION TIME RESPONSE

BLIIRA time-response measurements were performed with the same beam geometry as described above, except that IR light was not permitted to circulate inside

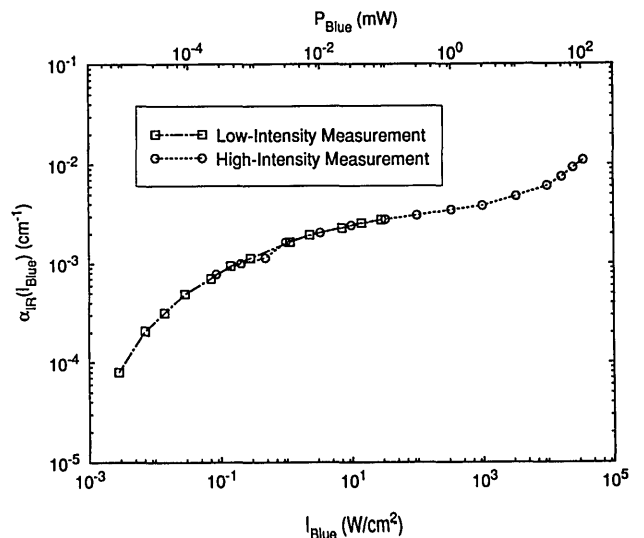
the cavity. Instead, a pick-off mirror was placed just downstream of the crystal to redirect the IR beam to a photodetector (see Fig. 2). By monitoring the IR transmission through the crystal while pulses of blue light were applied, we were able to investigate the buildup and recovery dynamics of BLIIRA.

The cw blue output of our doubling cavity was converted to a pulse train by a Pockels cell and acousto-optic modulator operated in series. This arrangement provided an extinction ratio of close to 10^{-5} , corresponding to dark levels below 1 μW . A very high degree of extinction was deemed necessary given the extreme sensitivity of KNbO_3 to even very small levels of blue light. We investigated BLIIRA dynamics with blue pulses of duration 5 μs to 100 ms, repetition rate 0.5 Hz to 3 kHz, and peak power 20–100 mW. We also varied the temperature of the crystal between room temperature and 90°C.

Figures 7 and 8 show typical graphs of IR transmission as a function of time. In each case the lower trace shows the instantaneous level of blue light, and the upper trace shows the induced dip in IR probe power arriving at the



(a)



(b)

Fig. 5. Plots showing the cw intensity dependence of BLIIRA in our best KNbO_3 crystal on (a) log–lin and (b) log–log scales.

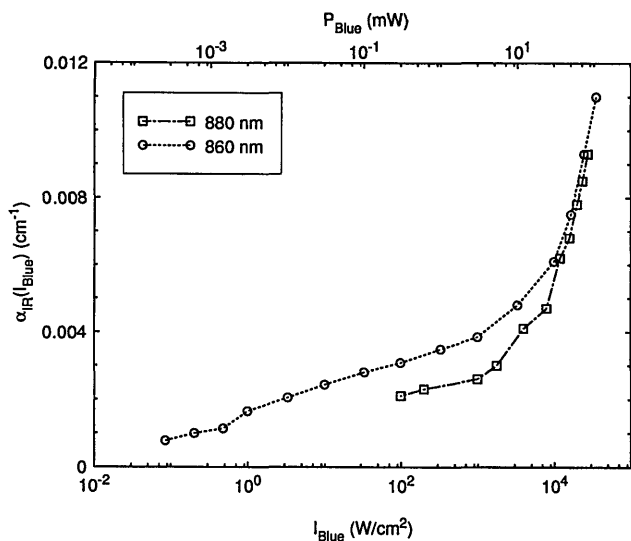


Fig. 6. Curves showing the cw intensity dependence of BLIIRA at IR wavelengths of 860 and 880 nm.

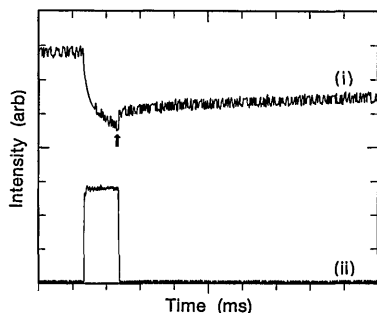


Fig. 7. Induced dip in IR transmission through the KNbO_3 ring cavity when the crystal is illuminated by 15-kW/cm^2 blue pulses (1-ms duration, 0.5-Hz repetition rate). The upper trace (i) shows the intensity of IR light reaching the detector as a function of time, and the lower trace (ii) shows the envelope of the blue pulse.

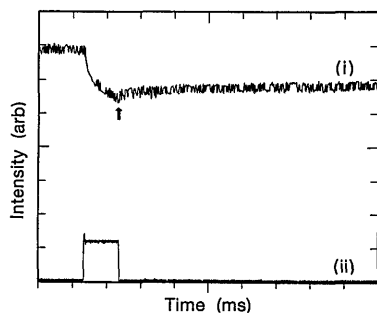


Fig. 8. Same as Fig. 7 but for blue pulses with peak intensity 7 kW/m^2 .

detector D in Fig. 2. The transmission dip for the IR exhibits both nonexponential buildup and nonexponential recovery. The peak value of IR absorption is close to the steady-state value observed for cw blue light with an intensity equal to the peak intensity of the blue pulse.

We attempted to characterize the time scale for BLIIRA buildup by measuring the peak light-induced IR absorption for blue pulses of very short duration. We found that the peak BLIIRA level dropped below measurement sen-

sitivity (approximately 0.1%) for blue pulses shorter than $5\ \mu\text{s}$ with a repetition rate below 30 Hz, suggesting that one can beat the effects of BLIIRA in our crystals by going to pulsed doubling or downconversion with low duty cycle. Unfortunately, our peak pulse intensity of approximately 15 kW/cm^2 corresponds to an average power of only $20\ \mu\text{W}$. In addition, because our measurements are made with a limited range of peak intensity and pulse length, it is not clear from our data how the buildup time scale depends on the peak pulse intensity. In particular it is certainly possible that our figure of $5\ \mu\text{s}$ might not be valid for pulses of the same energy but with shorter duration and higher peak intensity, such as those from a pulsed laser.

Another interesting result of our time-response measurements is that the shape of the trailing edge of the IR transmission dip depends quite strongly on the peak intensity of the blue pulse. Figures 7 and 8 show transmission dips induced by blue pulses of 15 and 7 kW/cm^2 (1-ms duration, 0.5-Hz repetition rate). Although the first trace transmission dip has a sharp initial step in its trailing edge (indicated by the arrow in Fig. 7), in the second trace this step is hardly seen. As previously noted for our cw measurements, a significant increase in the slope of the BLIIRA intensity dependence (Fig. 5) occurs in the vicinity of 5 kW/cm^2 . We suggest that this change in slope is due to the activation of a secondary BLIIRA mechanism. Because the measurements with pulsed blue light were performed in the intensity regime near the same threshold of the hypothetical secondary BLIIRA mechanism, it is tempting to associate the sharp step in Fig. 7 with this secondary mechanism.

As mentioned above, the recovery from BLIIRA is highly nonexponential. In fact, we recorded many traces for which the trailing edge of the transmission dip fits well to a logarithm (Fig. 9). This feature is responsible for low-duty cycles needed to avoid that effect of integrating BLIIRA when even very short pulses are used.

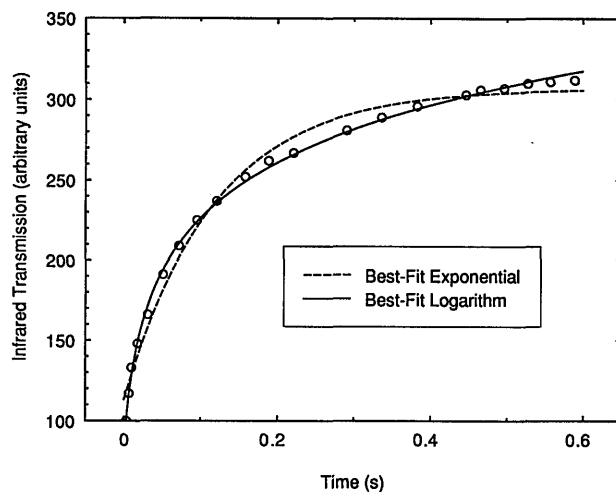


Fig. 9. Nonexponential recovery of IR transmission after a KNbO_3 crystal is illuminated with a pulse of blue light (intensity, 12 kW/cm^2 , duration, 100 ms; repetition rate, 0.5 Hz). This plot shows the level of IR power arriving at the detector D as a function of time (see Fig. 2) as well as the best-fit exponential and logarithmic curves. The point $t = 0$ on the x axis corresponds to the trailing edge of the blue pulse.

Processes that evolve logarithmically with time (creep phenomena) are generally associated with thermal activation over an ensemble of potential barriers with broadly distributed heights.¹⁷ One can easily envision such a situation within the context of the charge-transport model of light-induced absorption. In this model the recovery from BLIIRA is associated with thermal ionization of charge carriers from shallow traps; if the depth of these traps is not well defined but rather is inhomogeneously broadened, one might expect that the recovery would be logarithmic when it is viewed on certain time scales determined by the distribution of trap depths.¹⁷

5. DISCUSSION

As mentioned in previous sections, the salient features of our data can be understood quite simply (in qualitative terms) if one assumes a slightly modified version of the two-center charge-transport model for light-induced absorption.¹¹ However, in the absence of quantitative comparisons (which are beyond the scope of this research), we do not feel that our results in any way verify the charge-transport model of light-induced absorption; we include this discussion with the intent of suggesting directions for further investigation.

As applied to our situation, the two-center charge-transport model amounts to the following (see Fig. 10). Midgap impurities in KNbO_3 act as deep or shallow traps for holes, which are known to be the dominant charge carriers in undoped KNbO_3 .² The shallow charge carriers in undoped KNbO_3 .² The shallow traps are supposed to be shallow enough that thermal ionization keeps them completely empty at normal operating temperatures in the absence of blue light. Illumination by blue light causes photoionization of holes from deep traps [Fig. 11(a)], thereby increasing the concentration of holes in the valence band. Those holes can fall into shallow traps. If their concentration is sufficiently high, the recombination rate can overcome the thermal ionization rate, resulting in the buildup of a nonzero steady-state population of holes in shallow traps [Fig. 11(b)]. If we assume that IR photons are of insufficient energy to photoionize holes from the deep traps but that they can interact with holes in shallow traps, we then have a mechanism for BLIIRA.

The modification to the two-center model that we propose for the interpretation of our data is simply the addition of a third, very shallow trapping level (Fig. 12). The existence of such an additional level provides a straightforward explanation for the division of the BLIIRA cw intensity-dependence curve into low- and high-intensity regimes. The thermal ionization rate of the very shallow trap should be large compared with that of the original shallow trap. Therefore the very shallow traps should not be populated by holes unless the valence-band concentration of holes (i.e., the blue intensity) is very high. The secondary BLIIRA threshold occurring near 5 kW/cm^2 (Fig. 5) might thus be associated with the activation of this very shallow trap for IR absorption. With regard to the wavelength dependence of BLIIRA shown in Fig. 6, one could speculate that 880-nm IR light might be absorbed at very shallow traps just as strongly as the 860-nm IR light is but that the interaction cross-section

for 880-nm IR light with the original shallow traps is somewhat smaller than that for 860-nm IR light.

As for the time response implied by this model, the component of BLIIRA associated with absorption at very shallow traps should decay quickly owing to the high thermal ionization rate of these traps. Hence, the presence of very shallow trapping centers can also serve to explain the appearance of sharp steps observed in the trailing edge of IR transmission dips (see Fig. 7), as well as the variation of the size of these steps with the peak intensity of blue light.

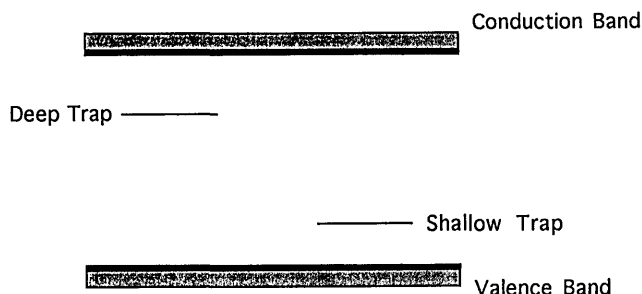


Fig. 10. Level diagram for the two-center charge-transport model of BLIIRA.

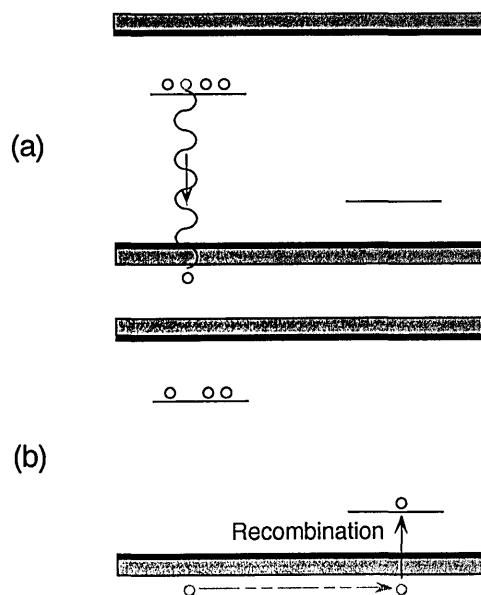


Fig. 11. Schematic of the BLIIRA process (see text).

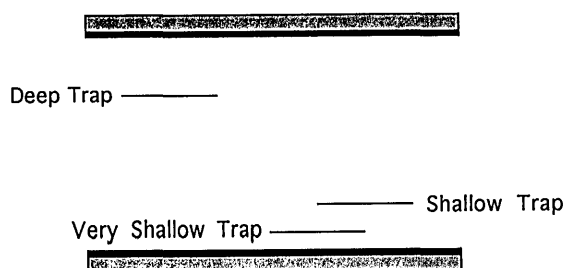


Fig. 12. Proposed modification to the two-center charge-transport model involving the addition of a third, very shallow trapping center.

6. SUMMARY

We regard the main results of this research to be the BLIIRA cw intensity-dependence curves shown in Figs. 3–6 and the general characterization of BLIIRA dynamics. By making precise measurements of BLIIRA in beam geometries identical to those used for frequency doubling and parametric oscillation, we have been able to verify directly that BLIIRA principally accounts for the anomalous intracavity losses that are implied by our measurements of conversion efficiency and OPO threshold in an ultra-low-loss ring cavity with KNbO_3 . We have also determined that it should be possible to circumvent the deleterious effects of BLIIRA by the use of pulsed doubling or parametric oscillation, although with low duty cycle and average power.

ACKNOWLEDGMENTS

We acknowledge the assistance of Nikos Georgiades and stimulating discussions with Sergei Orlov, who first suggested the use of a third trapping level to incorporate our results into the charge-transport model of light-induced absorption. We also thank Greg Mizell of Virgo Optics for helpful discussions and the generous loan of many KNbO_3 crystals used in this study. This research was funded by the U.S. Office of Naval Research and by the National Science Foundation.

REFERENCES

1. P. Günter and F. Micheron, "Photorefractive effects and photocurrents in $\text{KNbO}_3:\text{Fe}$," *Ferroelectrics* **18**, 27–38 (1978). See also P. Günter and J.-P. Huignard, eds., *Photorefractive Materials and Their Applications* (Springer-Verlag, Heidelberg, 1988).
2. R. J. Reeves, M. G. Jani, B. Jassemnejad, R. C. Powell, G. J. Mizell, and W. Fay, "Photorefractive properties of KNbO_3 ," *Phys. Rev. B* **43**, 71–82 (1991).
3. J. C. Bammert, J. Hoffnagle, and P. Günter, "High-efficiency intracavity frequency doubling of a Styryl-9 dye laser with KNbO_3 crystals," *Appl. Opt.* **24**, 1299–1301 (1985).
4. W. J. Kozlovsky, W. Lenth, E. E. Latta, A. Moser, and G. L. Bona, "Generation of 41 mW of blue radiation by frequency doubling of a GaAlAs diode-laser," *Appl. Phys. Lett.* **56**, 2291–2292 (1990).
5. M. K. Chun, L. Goldberg, I. N. Duling III, and T. F. Carruthers, in *Conference on Lasers and Electro-Optics*, Vol. 7 of 1990 OSA Technical Digest Series (Optical Society of America, Washington, D.C., 1990), paper CWE2.
6. E. S. Polzik and H. J. Kimble, "Frequency doubling with potassium niobate in an external cavity," in *Inorganic Crystals for Optics, Electrooptics, and Frequency Conversion*, P. F. Bordui, ed., *Proc. Soc. Photo-Opt. Instrum. Eng.* **1561**, 143–146 (1991).
7. E. S. Polzik and H. J. Kimble, "Frequency doubling with KNbO_3 in an external cavity," *Opt. Lett.* **16**, 1400–1402 (1991).
8. E. S. Polzik, H. Mabuchi, and H. J. Kimble, "Optical parametric oscillator with KNbO_3 and the process of light induced absorption," in *Conference on Lasers and Electro-Optics*, Vol. 11 of 1993 OSA Technical Digest Series (Optical Society of America, Washington, D.C., 1993), paper CThK6.
9. E. S. Polzik, J. Carri, and H. J. Kimble, "Spectroscopy with squeezed light," *Phys. Rev. Lett.* **68**, 3020–3023 (1992); "Atomic spectroscopy with squeezed light for sensitivity beyond the vacuum-state limit," *Appl. Phys. B* **55**, 279–290 (1992).
10. A. Ashkin, G. D. Boyd, and T. M. Dziedzic, "Resonant optical second harmonic generation and mixing," *IEEE J. Quantum Electron.* **QE-2**, 109–124 (1966).
11. F. Jermann and E. Krätzig, "Charge transport processes in $\text{LiNbO}_3:\text{Fe}$ at high intensity laser pulses," *Appl. Phys. A* **55**, 113–118 (1992).
12. P. Ye, A. Blouin, C. Demers, M.-M. D. Roberge, and X. Wu, "Picosecond photoinduced absorption in photorefractive BaTiO_3 ," *Opt. Lett.* **16**, 980–982 (1991).
13. K. Buse and E. Krätzig, "Light-induced absorption in BaTiO_3 and KNbO_3 generated with high intensity laser pulses," *Opt. Mat.* **1**, 165–170 (1992).
14. A. Motes and J. J. Kim, "Intensity-dependent absorption coefficient in photorefractive BaTiO_3 crystals," *J. Opt. Soc. Am. B* **4**, 1379–1381 (1987); A. Motes, G. Brost, J. Rotgé, and J. J. Kim, "Temporal behavior of the intensity-dependent absorption in photorefractive BaTiO_3 ," *Opt. Lett.* **13**, 509–511 (1988); G. A. Brost, R. A. Motes, and J. R. Rotgé, "Intensity-dependent absorption and photorefractive effects in barium titanate," *J. Opt. Soc. Am. B* **5**, 1879–1885 (1988); L. Holtmann, "A model for the nonlinear photoconductivity of BaTiO_3 ," *Phys. Status Solidi A* **113**, K89–K93 (1989); L. Holtmann, M. Unland, E. Krätzig, and G. Godefroy, "Conductivity and light-induced absorption in BaTiO_3 ," *Appl. Phys. A* **51**, 13–17 (1990); R. S. Cudney, R. M. Pierce, G. D. Bacher, and J. Feinberg, "Absorption gratings in photorefractive crystals with multiple levels," *J. Opt. Soc. Am. B* **8**, 1326–1332 (1991).
15. L. Holtmann, K. Buse, G. Kuper, A. Groll, H. Hesse, and E. Krätzig, "Photoconductivity and light-induced absorption in $\text{KNbO}_3:\text{Fe}$," *Appl. Phys. A* **53**, 81–86 (1991).
16. R. W. Drever, J. L. Hall, F. V. Kowalski, J. Hough, G. M. Ford, A. G. Munley, and H. Ward, "Laser phase and frequency stabilization using an optical resonator," *Appl. Phys. B* **31**, 97–105 (1983).
17. R. Street and J. C. Woolley, "A study of magnetic viscosity," *Proc. Phys. Soc. A* **62**, 562–572 (1949); M. Földéaki, L. Köszei, and R. A. Dunlap, "Time-dependent magnetic response in solids: phenomenology and physical background," *Philos. Mag. B* **63**, 1101–1117 (1991).